Translational Oncology 14 (2021) 101180

Contents lists available at ScienceDirect

Translational Oncology

journal homepage: www.elsevier.com/locate/tranon

Original Research

Early risk-assessment of patients with nasopharyngeal carcinoma: the added prognostic value of MR-based radiomics

Min-Jung Kim [a], Yangsean Choi [a,*], Yeoun Eun Sung [b], Youn Soo Lee [b], Yeon-Sil Kim [c], Kook-Jin Ahn [a], Min-Sik Kim [d]

[a] Department of Radiology, Seoul St. Mary's Hospital, College of Medicine, The Catholic University of Korea, Seoul, Republic of Korea
[b] Department of Hospital Pathology, Seoul St. Mary's Hospital, College of Medicine, The Catholic University of Korea, Seoul, Republic of Korea
[c] Department of Radiation Oncology, Seoul St. Mary's Hospital, College of Medicine, The Catholic University of Korea, Seoul, Republic of Korea
[d] Department of Head and Neck Surgery, Seoul St. Mary's Hospital, College of Medicine, The Catholic University of Korea, Seoul, Republic of Korea

ARTICLE INFO

Keywords:
Magnetic resonance imaging
Prognosis
Nasopharyngeal carcinoma
Progression-free survival

ABSTRACT

Objectives: To assess the additive prognostic value of MR-based radiomics in predicting progression-free survival (PFS) in patients with nasopharyngeal carcinoma (NPC)

Methods: Patients newly diagnosed with non-metastatic NPC between June 2006 and October 2019 were retrospectively included and randomly grouped into training and test cohorts (7:3 ratio). Radiomic features (n=213) were extracted from T2-weighted and contrast-enhanced T1-weighted MRI. The patients were staged according to the 8th edition of American Joint Committee on Cancer Staging Manual. The least absolute shrinkage and selection operator was used to select the relevant radiomic features. Univariate and multivariate Cox proportional hazards analyses were conducted for PFS, yielding three different survival models (clinical, stage, and radiomic). The integrated time-dependent area under the curve (iAUC) for PFS was calculated and compared among different combinations of survival models, and the analysis of variance was used to compare the survival models. The prognostic performance of all models was validated using a test set with integrated Brier scores.

Results: This study included 81 patients (training cohort=57; test cohort=24), and the mean PFS was 57.5 ± 43.6 months. In the training cohort, the prognostic performances of survival models improved significantly with the addition of radiomics to the clinical (iAUC, 0.72–0.80; p=0.04), stage (iAUC, 0.70–0.79; p=0.001), and combined models (iAUC, 0.76–0.81; p<0.001). In the test cohort, the radiomics and combined survival models were robustly validated for their ability to predict PFS.

Conclusion: Integration of MR-based radiomic features with clinical and stage variables improved the prediction PFS in patients diagnosed with NPC.

Introduction

Nasopharyngeal carcinoma (NPC) is a distinct subset of head and neck cancer endemic to Southeast Asia and Southern China, with a reported incidence rate of 50–80 cases per 100,000 people per year [1]. The standard treatment for NPC is concurrent chemoradiotherapy with or without adjuvant chemotherapy, which has led to substantial improvement in overall survival in patients with advanced NPC [2].

Although treatment decisions are primarily based on the tumor-nodule-metastasis (TNM) stage [3], its role in predicting prognosis may be limited [4]. Moreover, the early identification of unfavorable treatment outcomes could aid in more individualized clinical decisions prior to initiating treatment. Currently, the plasma load of Epstein-Barr virus (EBV) DNA is the only prognostic biomarker applicable in advanced-stage NPC [5] however, its prognostic value has been inconsistent [6]. Therefore, exploring other prognostic non-invasive

Abbreviations: AJCC, American Joint Committee on Cancer; CE-T1WI, Contrast-enhanced T1-weighted image; EBV, Epstein-Barr virus; iAUC, Integrated time-dependent area under the ROC curve; LASSO, Least absolute shrinkage and selection operator; NPC, Nasopharyngeal carcinoma; PFS, Progression-free survival; T2WI, T2-weighted image; TNM, Tumor-node-metastasis.

* Corresponding author.
E-mail address: phillipchoi007@gmail.com (Y. Choi).

https://doi.org/10.1016/j.tranon.2021.101180
Received 9 June 2021; Received in revised form 4 July 2021; Accepted 13 July 2021

biomarkers would be clinically relevant for risk stratification of patients diagnosed with NPC.

Several studies have investigated the role of diffusion-weighted MRI in predicting treatment response [7, 8] or distant metastasis [9] in NPC patients, thereby demonstrating the potential of diffusion-weighted MRI as a non-invasive prognostic imaging technique. More recently, radiomics, an emerging field for extracting high-throughput quantitative data from medical images, has shown promise in the prognostication of NPC [10–13]. Wang *et al.* explored the capability of MR-based radiomics to predict early treatment response to induction chemotherapy in patients with stage II–IV NPC [12]; they found that the radiomic signature demonstrated good predictive performance. However, the study was not inclusive of all cancer stages of NPC and only focused on treatment response to induction therapy.

The current study aims to expand the role of MR-based radiomics in patients with all stages of NPC, with progression-free survival (PFS) as the primary endpoint. Therefore, the purpose of the present study is to assess the additive prognostic value of radiomics when integrated with clinical and stage variables in predicting PFS in patients with NPC.

Materials and Methods

This single-center retrospective cohort study was approved by the Institutional Review Board of our institution, and informed consent was waived.

Patients

Patients diagnosed with NPC between June 2006 and October 2019 were retrospectively reviewed for inclusion. The inclusion criteria were as follows: 1) pathologically diagnosed with NPC at our institution; 2) available initial MRI prior to treatment; 3) available MR sequences, including T2-weighted images (T2WI) and contrast-enhanced T-weighted images (CE-T1WI); 4) received treatment at our institution; 5) age 18 years or older; and 6) absence of distant metastasis or secondary malignancy at initial presentation. Clinical information was retrieved from the electronic medical records maintained by our institution. Patients were grouped into training and test sets (7:3 ratio) via random stratified sampling such that the progression statuses were equally maintained between both sets (*caret* R package). The patients were staged according to the 8th edition of the American Joint Committee on Cancer (AJCC) TNM staging manual [14]. The histological subtypes of NPC were classified as follows based on the World Health Organization standard: 1) differentiated keratinizing carcinoma (type I), 2) differentiated non-keratinizing carcinoma (type II), and 3) undifferentiated non-keratinizing carcinoma (type III) [15]. A flowchart of the patient selection process is depicted in Fig. 1.

Progression-free survival

PFS was defined in this study as the interval between the initial date of pathological diagnosis and the date of disease progression, death, or last clinical visit in cases where no progression was observed. Disease progression was determined based on pathologic confirmation or obvious progression on clinical and imaging follow-up. Patients without disease progression were followed up for at least three months. The last follow-up date was December 29, 2020.

MRI acquisition

Two different 3.0-T MR scanners were used to acquire MRI scans of all patients (Verio, Siemens Healthineers with 16-channel head coils; Ingenia, Philips Healthcare with 32-channel head coils). Axial CE-T1WI images were acquired after administration of gadolinium-based contrast agent (Gadobutrol, Gadovist; Bayer Schering Pharma AG) at 0.01 mmol/kg. The acquisition protocols of neck MRI were slightly variable, but mostly consisted of the following parameters: 1) axial T2WI: repetition time/echo time [TR/TE] = 3600/82 ms, field of view [FOV] = 200 × 200, matrix = 320 × 256, flip angle = 160°, number of excitations = 1, echo train length = 15, slice thickness = 5 mm, gap = 5.75 mm, and 2) CE-T1WI: TR/TE = 603 × 16, FOV = 200 × 200, matrix = 320 × 256, flip angle = 150°, number of excitations = 1, echo train length = 5, slice thickness = 5 mm, gap = 5.75 mm).

MRI preprocessing and image segmentation

At first, both T2WI and CE-T1WI were co-registered using "General Registration" module in 3D Slicer (version 4.10.1, www.slicer.org) [16, 17]. MRI may be susceptible to artifacts of non-uniform intensity across the same type of tissue. To resolve this, N4 bias field correction was

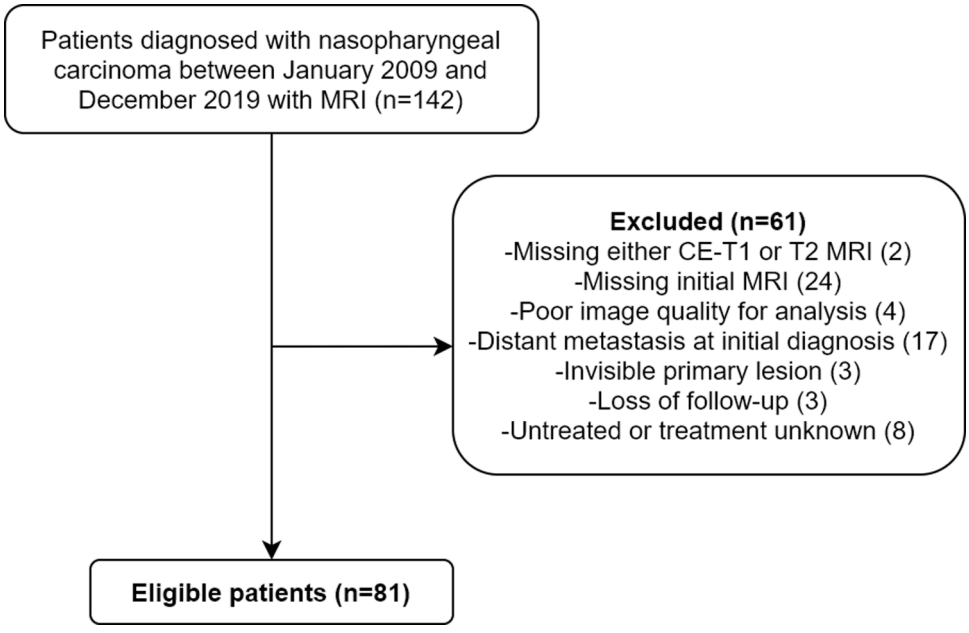

Fig. 1. Flowchart illustrating the patient selection process

applied to the original MRI using "N4ITK MRI Bias Field Correction" module in 3D Slicer [18], thereby improving intensity inhomogeneity across different MRIs. Furthermore, intensity normalization was performed from 0 to 255 using the PyRadiomics platform implanted in the 3D Slicer software [19].

Two radiologists with 7 and 8 years of experience in diagnostic head and neck radiology segmented the primary NPC in consensus. The segmentations included every axial slice with a visible primary tumor to obtain full three-dimensional ROIs (Fig. 2).

Radiomics feature extraction and selection

A total of 213 radiomic features were extracted from volumetric segmentations of both T2WI and CE-T1WI, and a heatmap of all radiomic features of patients is shown in Supplementary Fig. 1. In the training cohort, dimensionality reduction was performed via the least absolute shrinkage and selection operator (LASSO) with Cox regression [20], in which the optimal tuning parameter lambda (i.e., lambda.min, giving the minimal mean squared error) was identified after 10-fold cross validation [21] (*glmnet* R package).

Risk stratification of patients according to radscore

The radiomics score (radscore) was computed as the linear sum of the selected radiomic features with their respective coefficients weighted by Cox proportional hazards models of the training cohort as follows [22]:

$$1^{st}\text{featurecoefficient} \times 1^{st}\text{featurevalue} + \ldots + n^{th}\text{featurecoefficient} \times n^{th}\text{featurevalue}$$

The computed radscores were then dichotomized by optimal stratification based on log-rank statistics that yielded the most significant differences in PFS [23] (*survminer* R package).

Statistical analysis

All statistical analyses were performed using the R Statistical Software (version 3.5.1, Vienna, Austria). Student's *t*-test and chi-square test were used to compare continuous and categorical clinical variables, respectively, between the training and test cohorts. From the training cohort, univariate Cox proportional hazards analyses were used to calculate hazard ratios (HRs) with 95% confidence intervals (CIs) for the association between clinical, stage, radiomic covariates, and PFS. Multivariate Cox proportional hazards analyses were then performed to create the prognostic models (i.e., clinical, stage, radiomic, and combinations of each model). For each survival model, the integrated time-dependent area under the ROC curve (iAUC) was estimated, providing accuracy measures with respect to time-specific versions of sensitivity and specificity calculated from time-to-event data (*risksetROC* R package) [24]. The differences in iAUC between the survival models were calculated via bootstrapped resampling with 1000 repetitions. A statistically significant difference in iAUC was considered when the 95% CI did not contain zero. Additionally, analysis of variance was used to assess improvements in the survival models. The prognostic performance of all models was assessed in a test cohort using the prediction error curves of Brier scores over PFS times (*pec* R package). Finally, a nomogram for predicting 2- and 5-year PFS was plotted using *the rms* R package. All statistical tests were two-sided, and statistical significance was set at $p < 0.05$.

Results

Patients

The baseline characteristics of the patients are summarized in Table 1.

Among the 81 patients, the mean age was 53 ± 13 years, and there were 61 men (75.3%). The most common stage was 1 for both T-stage (38/81, 46.9%) and N-stage (36/81, 44.4%). AJCC stage III was the most prevalent disease (35/81, 43.2%), and the most common histological subtype was undifferentiated non-keratinizing carcinoma (49/81, 60.5%). Within the median follow-up period of 53 months (interquartile range=25–88 months), 16 deaths (19.8%), 3 local recurrences (3.7%), and 12 (14.8%) distant metastases were reported. The mean PFS was 57.5 ± 43.6 months. There were no significant differences in baseline covariates between the training (n=57) and test (n=24) cohorts (Supplementary Table 1).

Selected radiomic features and radscore

Seven radiomic features were selected, of which four features were extracted from CE-T1WI (Maximum2DDiameterSlice, ZoneVariance, LargeAreaEmphasis, SmallAreaEmphasis), and three from T2WI (Maximum2DDiameterSlice, Correlation, informational measure of correlation). Detailed descriptions and coefficients are provided in Supplementary Table 2 The dichotomization of patients into high-risk (n=29) and low-risk (n=52) groups according to the optimal stratification based on log-rank statistics of radscores is illustrated in Supplementary Fig. 2.

Prognostic models for progression-free survival

All Cox proportional hazards analyses were performed in the training cohort. In univariate Cox proportional hazards analysis, only the high-risk group based on radscore was significantly associated with poor PFS (HR=5.87; 95%; CI=1.55, 22.2; p=0.01) (Table 2).

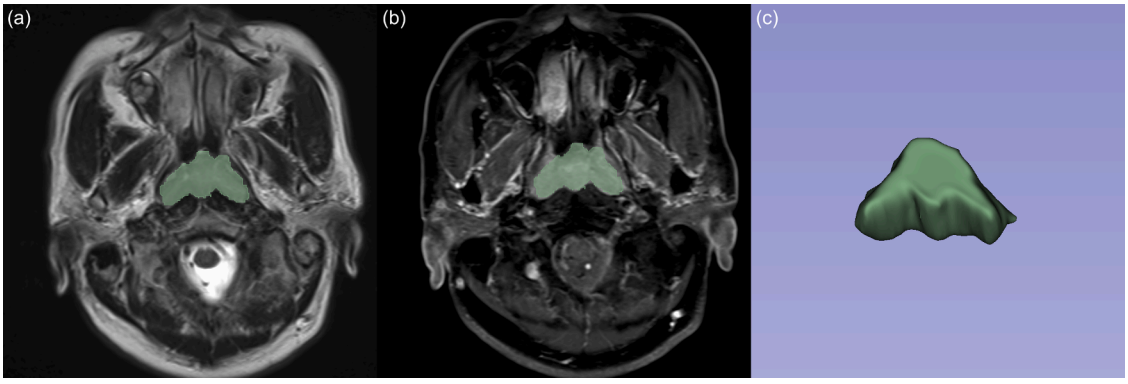

Fig. 2. Representative example MRI-based volumetric region of interest segmentation in a 58-year-old male patient on axial (a) T2WI, (b) CE-T1WI and (c) its three-dimensional reconstruction.

Table 1
Baseline characteristics of patients.

Covariate	n=81
Age, mean±SD	53±13
Sex, n (%)	
Male	61 (75.3)
Female	20 (24.7)
Smoking history, n (%)	
No	34 (42)
Yes	46 (56.8)
Unknown	1 (1.2)
T-stage, n (%)	
1	38 (46.9)
2	9 (11.1)
3	23 (28.4)
4	11 (13.6)
N-stage, n (%)	
0	12 (14.8)
1	36 (44.4)
2	29 (35.8)
3	4 (4.9)
AJCC 8th TNM stage, n (%)	
I	6 (7.4)
II	25 (30.9)
III	35 (43.2)
IVA	15 (18.5)
GTV (mL), mean±SD	15876±12976
Histologic subtype, n (%)	
Differentiated non-keratinizing carcinoma	27 (32.3)
Undifferentiated non-keratinizing carcinoma	49 (60.5)
Keratinizing squamous cell carcinoma	5 (6.2)
EBV status, n (%)	
Positive	53 (65.4)
Negative	12 (14.8)
Unknown	16 (19.8)
CCRT, n (%)	
Yes	74 (91.4)
No	7 (8.6)
Cumulative radiation dose (Gy), mean±SD	7002 ± 304
Clinical endpoints, n (%)	
Deaths	16 (19.8)
Local-recurrence	3 (3.7)
Distant metastasis	12 (14.8)
Progression-free survival (months), mean±SD	57.5 ± 43.6
Follow-up time (months), median (IQR)	52.7 (24.8–88.1)

Table 2
Univariate Cox proportional hazards analyses for progression-free survival.

Covariate	HR	95% CI	*P*-value
Age	1.05	0.99–1.1	0.10
Sex, male	3.81	4.88–29.8	0.20
Smoking, smoker	0.99	0.42–2.3	0.98
T-stage, 3-4	2.23	0.65–7.6	0.20
N-stage, 3-4	2.39	0.70–8.2	0.17
AJCC stage, III-IV	5.49	0.70–42.9	0.10
Cumulative radiation dose, >median	1.46	0.42–5.0	0.55
GTV, >median	0.74	0.22–2.4	0.62
Radscore, high-risk	5.87	1.55–22.2	0.01

AJCC, American Joint Committee on Cancer; GTV, gross tumor volume

Among the clinical variables, male sex (HR=3.81; 95% CI, 4.88–29.8), advanced T-stage (HR=2.23; 95% CI=0.65, 7.6), advanced N-stage (HR=2.39; 95% CI=0.7, 8.2), and advanced AJCC stage (HR=5.49; 95% CI=0.7, 42.9) were associated with poor PFS but without statistical significance (all, p>0.05). Cox proportional hazards analysis of 45 patients with known EBV status yielded an implausibly large coefficient with 95% CI ranging from zero to infinity, thus rendering unreliable results.

In multivariate survival models for PFS, the addition of stage variables to the clinical model did not significantly improve prognostic performance (Table 3) (p=0.43).

However, the addition of radiomic model to either clinical or stage model significantly improved their prognostic performances, yielding iAUC increments of 0.08 and 0.09, respectively. The addition of radiomic model to the combined clinical and stage model demonstrated the highest iAUC of 0.81 (95% CI=0.80, 0.81), with an iAUC increment of 0.04. The iAUC of all survival models are depicted in Fig. 3.

Finally, a nomogram with all variables was created visually to quantify the probability of 2-year and 5-year PFS (Fig. 4).

Table 3
Multivariate survival models for progressive-free survival.

Model layers	iAUC	95% CI	iAUC difference	95% CI	*P*-value *
Clinical**	0.72	0.71–0.73			
Stage***	0.70	0.69–0.71			
Radiomic	0.71	0.71–0.72			
Clinical + stage	0.76	0.75–0.77	0.04	0.03–0.05	0.43
Clinical + radiomic	0.80	0.79–0.80	0.08	0.07–0.09	0.04
Stage + radiomic	0.79	0.78–0.80	0.09	0.08–0.10	0.001
Clinical + stage + radiomics	0.81	0.80–0.81	0.04	0.04–0.05	<0.001

* *P*-values calculated from analysis of variance
** Clinical model consists of age, sex, smoking history, and cumulative radiation dose
*** AJCC TNM stage

Validation based on integrated Brier scores with prediction error curves

The survival models were validated in a separate test set via integrated Brier scores and illustrated as prediction error curves (Supplementary Fig. 3). Compared to the reference curve of Kaplan–Meier survival estimation, the combined and radiomic models demonstrated lower prediction error rates (i.e., lower curves) over a follow-up PFS period of longer than 12-months.

Discussion

The current study investigated the potential additive prognostic value of radiomic features derived from pre-treatment conventional MR sequences (T2WI and CE-T1WI) in patients with NPC. Seven relevant radiomic features were selected to construct the radiomics survival model, which significantly improved prognostication when it was added to the well-known clinical and stage variables. The radiomic and combined survival models were also validated in the test cohort. Our findings demonstrate that MR-based radiomics may hold promise for aiding early risk stratification of patients with NPC.

Past studies have yielded important insights into the role of MR-based radiomics in the prognostication of NPC. Mao *et al.* [25] applied texture analysis to pre-treatment T2WI and CE-T1WI in NPC patients and found that a combination of CE-T1WI-based uniformity features with tumor volume and overall stage improved the predictive ability for PFS. More specifically, the two features selected from CE-T1WI in our study, 'LargeAreaEmphasis' and 'SmallAreaEmphasis', were indicative of coarse and fine textures, respectively [19]. The prognostic performance of the combined model (C-index: 0.794) in their study was also very similar to ours (iAUC=0.81). The main difference is that their study only applied texture analysis, while the current study comprehensively included various standardized features from a wider array of radiomics.

Our finding is consistent with several recent studies which found that an MR-based radiomics model improved prediction of disease-free survival/PFS [26–28] and overall survival [29, 30]. All these studies applied generally similar approaches of extracting multiparametric MR-based radiomics and integrating them to the conventional clinical variables in their prognostic models. The combined number of patients in these studies is large (>1,000) and patients were recruited in both endemic and non-endemic regions, further supporting the prognostic

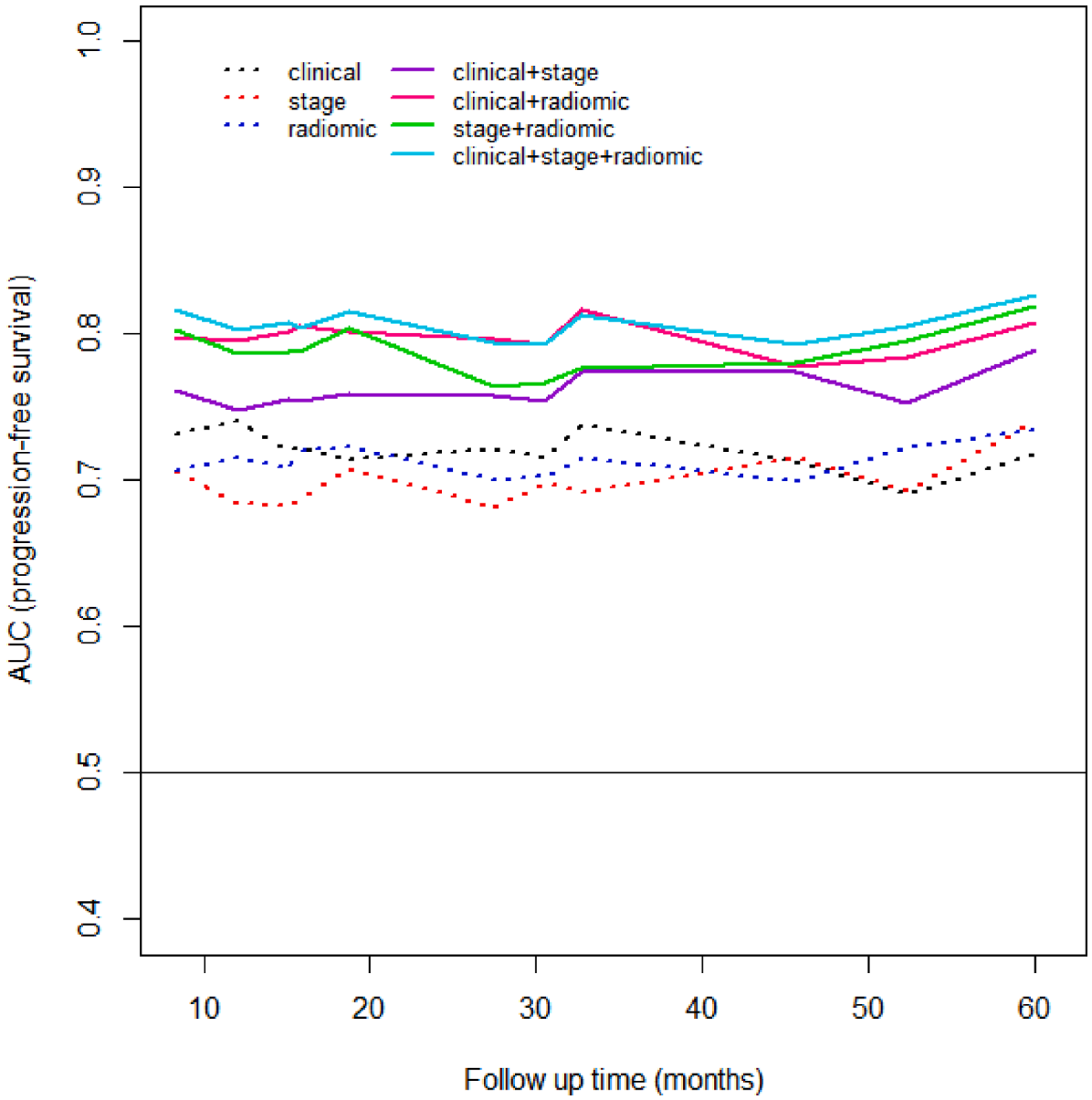

Fig. 3. Integrated AUC over progression-free survival times of different prognostic models.

role of MR-based radiomics in patients with NPC.

While positive EBV status is known to be associated with favorable overall survival [31] in patients with NPC, the clinical use of EBV-DNA levels for predicting prognosis has produced heterogeneous results in the past [6]. Likewise, our study did not reveal a meaningful prognostic value of EBV status in predicting PFS. This finding is in line with a study by Yip *et al.*, who reported that disease-free survival according to EBV status was not significantly different over long follow-up periods [31]. Radiomic features could be a reasonable alternative biomarker to EBV for patients with NPC, considering that they could be extracted non-invasively, and at a low cost.

For image analysis, we chose both T2WI and CE-T1WI for two reasons: 1) the two are the most commonly acquired conventional sequences during routine MRI scans, and thus might be more generalizable, 2) the radiomic features extracted from joint T2WI and CE-T1WI demonstrated better prognostic performance than those from single sequence [22]. Future research will have to investigate extracting radiomic features from advanced physiologic MR sequences, such as diffusion-weighted imaging or perfusion-weighted imaging, which might reveal interesting insights into the underlying prognostic value of radiomic features.

This study has several limitations. Firstly, the prognostic models were not externally validated in independent settings, limiting the generalizability of the results of the current study. Secondly, other detailed prognostic molecular biomarkers, such as c-Met, ERBB3, and MTDH [32]], were not investigated due to lack of data availability. Finally, PFS was not subcategorized into local recurrence-free survival or distant metastasis-free survival due to the small number of events for each subcategory.

In conclusion, the current study demonstrated that integrating MR-based radiomic features with well-known clinical variables improved prognostication of patients initially diagnosed with NPC. Our results provide evidence for the robust additive prognostic role of radiomics, which may aid in early clinical decision making.

CRediT authorship contribution statement

Min-Jung Kim: Formal analysis, Data curation. **Yangsean Choi:** Conceptualization, Methodology, Software, Formal analysis, Investigation, Resources, Data curation, Writing – original draft, Writing – review

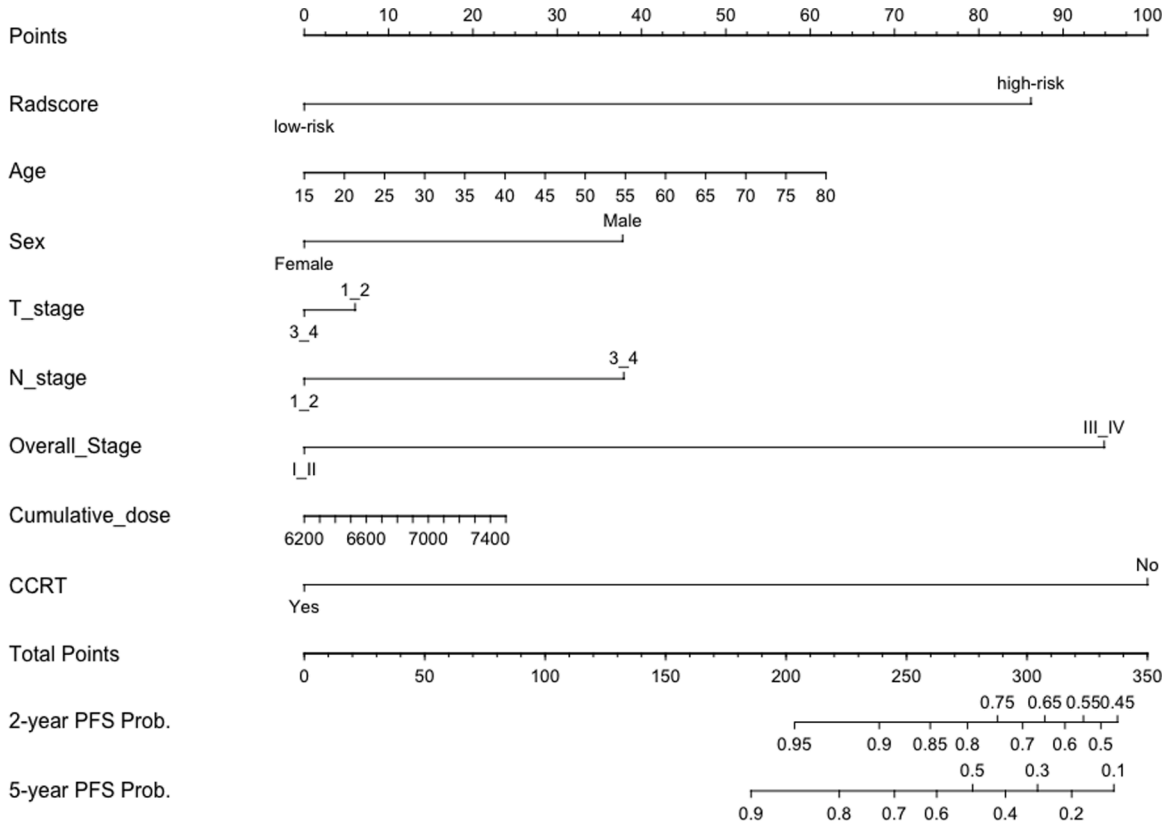

Fig. 4. Nomogram for predicting 2- and 5-year progression-free survival probability. The values of each variable are shown as points by projecting them onto the top line (point scale). Adding the points of all variables and projecting them downward to the bottom lines can calibrate the probabilities of 2-year and 5-year progression-free survival.

& editing, Visualization. **Yeoun Eun Sung:** Resources. **Youn Soo Lee:** Resources. **Yeon-Sil Kim:** Resources, Supervision. **Kook-Jin Ahn:** Resources, Supervision. **Min-Sik Kim:** Resources, Supervision.

Declaration of Competing Interest

The authors declare that they have no known competing financial interests or personal relationships that could have appeared to influence the work reported in this paper.

Acknowledgments

This research was supported by Basic Science Research Program through the National Research Foundation of Korea (NRF) funded by the Ministry of Education (2021R1I1A1A01040285)

Supplementary materials

Supplementary material associated with this article can be found, in the online version, at doi:10.1016/j.tranon.2021.101180.

References

[1] X An, FH Wang, PR Ding, et al., Plasma Epstein-Barr virus DNA level strongly predicts survival in metastatic/recurrent nasopharyngeal carcinoma treated with palliative chemotherapy, Cancer 117 (2011) 3750–3757, https://doi.org/10.1002/cncr.25932.
[2] P Blanchard, A Lee, S Marguet, et al., Chemotherapy and radiotherapy in nasopharyngeal carcinoma: an update of the MAC-NPC meta-analysis, Lancet Oncol. 16 (2015) 645–655, https://doi.org/10.1016/S1470-2045(15)70126-9.
[3] ATC Chan, V Grégoire, JL Lefebvre, et al., Nasopharyngeal cancer: EHNS-ESMO-ESTRO clinical practice guidelines for diagnosis, treatment andfollow-up, Ann. Oncol. 23 (2012) vii83–vii85, https://doi.org/10.1093/annonc/mds266.
[4] HY Wang, BY Sun, ZH Zhu, et al., Eight-signature classifier for prediction of nasopharnyngeal carcinoma survival, J. Clin. Oncol. 29 (2011) 4516–4525, https://doi.org/10.1200/JCO.2010.33.7741.
[5] SF Leung, KCA Chan, BB Ma, et al., Plasma Epstein-Barr viral DNA load at midpoint of radiotherapy course predicts outcome in advanced-stage nasopharyngeal carcinoma, Ann. Oncol. (2014), https://doi.org/10.1093/annonc/mdu117.
[6] J Zhang, C Shu, Y Song, et al., Epstein-Barr virus DNA level as a novel prognostic factor in nasopharyngeal carcinoma A meta-analysis, Med (United States) 95 (2016), https://doi.org/10.1097/MD.0000000000005130.
[7] WY Huang, MM Li, SM Lin, et al., In vivo imaging markers for prediction of radiotherapy response in patients with nasopharyngeal carcinoma: RESOLVE DWI versus DKI, Sci. Rep. 8 (2018) 1–8, https://doi.org/10.1038/s41598-018-34072-9.
[8] DF Yan, WB Zhang, SB Ke, et al., The prognostic value of pretreatment tumor apparent diffusion coefficient values in nasopharyngeal carcinoma, BMC Cancer 17 (2017) 4–11, https://doi.org/10.1186/s12885-017-3658-x.
[9] QY Ai, AD King, BKH Law, et al., Diffusion-weighted imaging of nasopharyngeal carcinoma to predict distant metastases, Eur. Arch. Oto-Rhino-Laryngol. 274 (2017) 1045–1051, https://doi.org/10.1007/s00405-016-4333-6.
[10] HJWL Aerts, ER Velazquez, RTH Leijenaar, et al., Decoding tumour phenotype by noninvasive imaging using a quantitative radiomics approach, Nat. Commun. (2014), https://doi.org/10.1038/ncomms5006.
[11] L Zhang, H Zhou, D Gu, et al., Radiomic nomogram: Pretreatment evaluation of local recurrence in nasopharyngeal carcinoma based on MR imaging, J. Cancer 10 (2019) 4217–4225, https://doi.org/10.7150/jca.33345.
[12] G Wang, L He, C Yuan, et al., Pretreatment MR imaging radiomics signatures for response prediction to induction chemotherapy in patients with nasopharyngeal carcinoma, Eur. J. Radiol. 98 (2018) 100–106, https://doi.org/10.1016/j.ejrad.2017.11.007.
[13] B Zhang, X He, F Ouyang, et al., Radiomic machine-learning classifiers for prognostic biomarkers of advanced nasopharyngeal carcinoma, Cancer Lett. 403 (2017) 21–27, https://doi.org/10.1016/j.canlet.2017.06.004.
[14] WM Lydiatt, SG Patel, B O'Sullivan, et al., Head and neck cancers-major changes in the American Joint Committee on cancer eighth edition cancer staging manual, CA Cancer J. Clin. 67 (2017) 122–137, https://doi.org/10.3322/caac.21389.
[15] J Huang, M Fogg, LJ Wirth, et al., Epstein-Barr virus-specific adoptive immunotherapy for recurrent, metastatic nasopharyngeal carcinoma, Cancer 123 (2017) 2642–2650, https://doi.org/10.1002/cncr.30541.
[16] A Fedorov, R Beichel, J Kalpathy-Cramer, et al., 3D Slicer as an image computing platform for the Quantitative Imaging Network, Magn. Reson. Imaging 30 (2012) 1323–1341, https://doi.org/10.1016/j.mri.2012.05.001.

[17] H Johnson, G Harris, K Williams, BRAINSFit: mutual information rigid registrations of whole-brain 3D images, using the insight toolkit, Insight. J. 57 (2007).
[18] NJ Tustison, JC Gee, N4ITK: Nick's N3 ITK implementation for MRI bias field correction, Insight. J. (2009) 1–8.
[19] JJM Van Griethuysen, A Fedorov, C Parmar, et al., Computational radiomics system to decode the radiographic phenotype, Cancer Res. 77 (2017) e104–e107, https://doi.org/10.1158/0008-5472.CAN-17-0339.
[20] R. Tibshirani, The lasso method for variable selection in the cox model, Stat. Med. 16 (1997) 385–395, https://doi.org/10.1002/(SICI)1097-0258(19970228)16:4<385::AID-SIM380>3.0.CO;2-3.
[21] W Sauerbrei, P Royston, H Binder, Selection of important variables and determination of functional form for continuous predictors in multivariable model building. Statistics in Medicine, 2007.
[22] B Zhang, J Tian, D Dong, et al., Radiomics features of multiparametric MRI as novel prognostic factors in advanced nasopharyngeal carcinoma, Clin. Cancer Res. 23 (2017) 4259–4269, https://doi.org/10.1158/1078-0432.CCR-16-2910.
[23] B Lausen, M Schumacher, Maximally selected rank statistics, Biometrics (1992) 73–85.
[24] P Blanche, JF Dartigues, H Jacqmin-Gadda, Estimating and comparing time-dependent areas under receiver operating characteristic curves for censored event times with competing risks, Stat. Med. 32 (2013) 5381–5397, https://doi.org/10.1002/sim.5958.
[25] J Mao, J Fang, X Duan, et al., Predictive value of pretreatment MRI texture analysis in patients with primary nasopharyngeal carcinoma, Eur. Radiol. 29 (2019) 4105–4113, https://doi.org/10.1007/s00330-018-5961-6.
[26] LZ Zhong, XL Fang, D Dong, et al., A deep learning MR-based radiomic nomogram may predict survival for nasopharyngeal carcinoma patients with stage T3N1M0, Radiother. Oncol. 151 (2020) 1–9, https://doi.org/10.1016/j.radonc.2020.06.050.
[27] L Zhao, J Gong, Y Xi, et al., MRI-based radiomics nomogram may predict the response to induction chemotherapy and survival in locally advanced nasopharyngeal carcinoma, Eur. Radiol. 30 (2020) 537–546, https://doi.org/10.1007/s00330-019-06211-x.
[28] H Shen, Y Wang, D Liu, et al., Predicting Progression-Free Survival Using MRI-Based Radiomics for Patients With Nonmetastatic Nasopharyngeal Carcinoma, Front. Oncol. 10 (2020) 618, https://doi.org/10.3389/fonc.2020.00618.
[29] X Ming, RW Oei, R Zhai, et al., MRI-based radiomics signature is a quantitative prognostic biomarker for nasopharyngeal carcinoma, Sci. Rep. 9 (2019) 10412, https://doi.org/10.1038/s41598-019-46985-0.
[30] M Bologna, V Corino, G Calareso, et al., Baseline MRI-radiomics can predict overall survival in non-endemic EBV-related nasopharyngeal carcinoma patients, Cancers (Basel) 12 (2020) 2958, https://doi.org/10.3390/cancers12102958.
[31] KW Yip, W Shi, M Pintilie, et al., Prognostic significance of the Epstein-Barr virus, p53, Bcl-2, and survivin in nasopharyngeal cancer, Clin. Cancer Res. 12 (2006) 5726–5732, https://doi.org/10.1158/1078-0432.CCR-06-0571.
[32] JP Bruce, K Yip, SV. Bratman, et al., Nasopharyngeal cancer: Molecular landscape, J. Clin. Oncol. 33 (2015) 3346–3355, https://doi.org/10.1200/JCO.2015.60.7846.